Numerical Heat Transfer, Part A: Applications: An International Journal of Computation and Methodology

Publication details, including instructions for authors and subscription information:
http://www.tandfonline.com/loi/unht20

Natural Convection in a Rectangular Enclosure with Sinusoidal Temperature Distributions on both Side Walls

Qi-Hong Deng [a] & Juan-Juan Chang [a]

[a] School of Energy Science and Engineering, Central South University, Changsha, Hunan, People's Republic of China

Published online: 30 Jul 2008.

To cite this article: Qi-Hong Deng & Juan-Juan Chang (2008) Natural Convection in a Rectangular Enclosure with Sinusoidal Temperature Distributions on both Side Walls, Numerical Heat Transfer, Part A: Applications: An International Journal of Computation and Methodology, 54:5, 507-524, DOI: 10.1080/01457630802186080

To link to this article: http://dx.doi.org/10.1080/01457630802186080

Numerical Heat Transfer, Part A, 54: 507–524, 2008

ISSN: 1040-7782 print/1521-0634 online
DOI: 10.1080/01457630802186080

Taylor & Francis
Taylor & Francis Group

NATURAL CONVECTION IN A RECTANGULAR ENCLOSURE WITH SINUSOIDAL TEMPERATURE DISTRIBUTIONS ON BOTH SIDE WALLS

Qi-Hong Deng and Juan-Juan Chang
School of Energy Science and Engineering, Central South University, Changsha, Hunan, People's Republic of China

A two-dimensional steady and laminar natural convection in an air-filled (Pr = 0.7) rectangular enclosure is investigated numerically. The horizontal walls are thermally insulated and the vertical side walls have two spatially varying sinusoidal temperature distributions of different amplitudes and phases. The governing equations in primitive variables are discretized by the finite-volume method and solved by the SIMPLE algorithm. The fluid flow and heat transfer characteristics are systematically investigated over a wide range of Rayleigh number (Ra = 10^3–10^6), amplitude ratio ($\varepsilon = 0 - 1$), phase deviation ($\phi = 0 - \pi$), and aspect ratio (Ar = 0.25–4). The results show that the natural-convection heat transfer in enclosures with two sinusoidal temperature distributions on the side walls is superior to that with a single sinusoidal temperature profile on one side wall.

INTRODUCTION

Natural convection in enclosures has received considerable attention in the past few decades, as comprehensively reviewed by Ostrach [1], and will continue to be an attractive and fundamental research field. One reason is its various engineering applications, such as solar energy systems, indoor thermal environments, nuclear reactor systems, cooling of electronic equipment, and various chemical and/or industrial processes. The other reason is the growing scientific research interest in heat transfer enhancement of natural convection in enclosures. For no operating cost or noise, natural convection usually provides a simple but effective approach to remove heat from enclosures, but the comparatively low heat transfer rate and large space requirement become the main limitations for its practical applications. How to increase heat transfer in enclosures so as to design smart but compact natural convection has become a main concern of recent years. Much focus has also been

Received 19 December 2007; accepted 25 April 2008.

The work was financially supported by the following projects: National Natural Science Foundation of China (50408019), Foundation for the Author of National Excellent Doctoral Dissertation of China (FANEDD 200545), Program for New Century Excellent Talents in University of China (NCET-05-0688), Fok Ying Tung Education Foundation (104006), Hunan Provincial Natural Science Foundation of China (06JJ1001).

Address correspondence to Qi-Hong Deng, School of Energy Science and Engineering, Central South University, Changsha, Hunan 410083, People's Republic of China. E-mail: qhdeng@csu.edu.cn

NOMENCLATURE

A	amplitude of the sinusoidal temperature function	u, v	dimensional velocity components in x and y directions
Ar	aspect ratio	U, V	dimensionless velocity components in X and Y directions
g	gravity acceleration		
H	height of the enclosure	x, y	dimensional coordinates
L	length of the enclosure	X, Y	dimensionless coordinates
n	normal direction of the surface	α	thermal diffusivity
Nu, $\overline{\text{Nu}}$	local and average Nusselt numbers	β	expansion coefficient
p, P	dimensional and dimensionless pressures	ε	amplitude ratio
		ν	kinematic viscosity
Pr	Prandtl number	ρ	density
Ra	Rayleigh number	ϕ	phase deviation
t, T	dimensional and dimensionless temperature	ψ	stream function
		Subscripts	
Δt	temperature scale	l	left wall
t_0	reference temperature	r	right wall

directed to the fundamental fluid flow and heat transfer characteristics under different boundary conditions.

In addition to conventional natural convection in enclosures with uniform thermal boundaries, recent attention has been intensively focused on the cases with nonuniform temperature distribution on the walls. The numerical studies on this topic are basically categorized into three classes. The first class is that one wall is divided into two zones of different temperatures. Poulikakos [2] studied a two-dimensional (2-D) enclosure with one vertical side wall differentially heated; one half of the wall is heated and the other half is cooled, and the remaining walls are insulated. Jahnke et al. [3] then investigated a 2-D enclosure with vertical side walls both differentially heated, the upper halves cooled and the lower halves heated. Fu et al. [4] considered a more complicated enclosure, with the heated wall of the enclosure divided into higher- and lower-temperature regions and the temperature of the cold wall maintained at a constant. The second nonuniform class is that the temperature along one wall is changed linearly. Oosthuizen [5] considered an enclosure with heating from the bottom surface and cooling from the top surface, and the side walls were maintained at a linearly varying temperature. Kumar and Singh [6] examined a porous rectangular enclosure with a linear temperature distribution on one side wall. Kumar and Shalini [7] later investigated a porous enclosure with one wavy side wall having a linear temperature profile. Recently, Sathiyamoorthy et al. [8, 9] studied a more complicated square cavity, filled with either fluid or a porous medium, with the temperature along both side walls varied linearly. The third class of natural convection in enclosures with nonuniform thermal boundaries is that the wall temperature is varied sinusoidally according to the space coordinate. Bilgen and Yedder [10] considered a 2-D rectangular enclosure with a sinusoidal temperature profile imposed on one vertical side wall and the other walls insulated. A similar work conducted by Sarris et al. [11] used a 2-D rectangular enclosure with the top wall heated with a sinusoidal temperature profile and all the other walls insulated. A porous rectangular enclosure with sinusoidal temperature distribution on the

bottom wall and adiabatic condition on the other walls was analyzed by Varol et al. [12]. Saeid and Yaacob [13] studied a square cavity with one side wall heated by a sinusoidal temperature profile, the other side wall cooled at a constant temperature, and the horizontal walls insulated. The corresponding case in a porous square cavity was studied by Saeid and Mohamad [14]. Basak et al. [15] considered a square cavity with the bottom wall heated sinusoidally, the vertical side walls both cooled at constant temperatures, and the top wall insulated. Dalal and Das [16] examined a rectangular cavity sinusoidally heated from below and uniformly cooled from the other walls. Recently, Dalal and Das [17, 18] considered an enclosure heated from the top surface with a sinusoidally varying temperature and cooled from the other three surfaces including one wavy vertical side wall.

Review of the above literatures found that the nonuniform thermal boundary has a significant effect on the natural convection in enclosures, resulting multicellular flow structures and more complicated heat transfer characteristics. Although the above studies varied from case to case, fundamental understanding of fluid flow and heat transfer characteristics of natural convection in enclosures with non-uniform thermal boundaries is still lacking, and more investigations are required. The present work aims to investigate a more complicated natural convection in an enclosure with two sinusoidal temperature profiles on the side walls. As expected, the interaction between the two sinusoidally varying temperatures creates new fluid flow and heat transfer characteristics. The results obtained indicate that the physical model offers a framework to increase heat transfer for natural convection in enclosures.

PHYSICAL MODEL

Figure 1 shows the physical model of the present study schematically. There is natural convection in an air-filled 2-D rectangular enclosure with length L and height H. The Cartesian coordinate system has its origin at the lower left corner of the enclosure, and the orientations of the x and y axes are along the length and height of the enclosure, respectively. The gravitational acceleration acts in the reverse direction of the y coordinate. The horizontal top and bottom walls are thermally

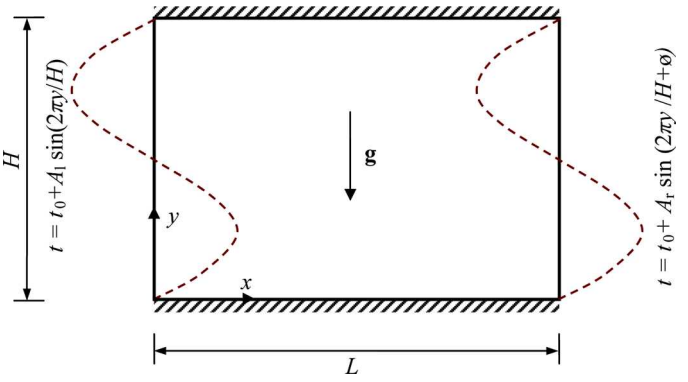

Figure 1. Schematic model of natural convection in a 2-D rectangular enclosure with sinusoidal temperature distributions on side walls (figure is provided in color online).

insulated, but the left and right vertical side walls have imposed two sinusoidally varying temperature distributions according to the space coordinate as follows:

$$\begin{aligned} t(y) &= t_0 + A_l \sin\left(\frac{2\pi y}{H}\right) \qquad \text{at } x = 0 \\ t(y) &= t_0 + A_r \sin\left(\frac{2\pi y}{H} + \phi\right) \quad \text{at } x = L \end{aligned} \tag{1}$$

where the reference/mean temperatures of the sinusoidal temperature profiles on the left and right side walls are the same as t_0, but the amplitude and phase of the sinusoidal profiles are, respectively, A_l and 0, and A_r and ϕ.

MATHEMATICAL MODEL

The natural convection is considered to be incompressible, steady, and laminar, and the Boussinesq approximation is employed to account for the thermal buoyancy effects. The governing equations in dimensionless form are as follows.
Continuity:

$$\frac{\partial U}{\partial X} + \frac{\partial V}{\partial Y} = 0 \tag{2}$$

Momentum:

$$U\frac{\partial U}{\partial X} + V\frac{\partial U}{\partial Y} = -\frac{\partial P}{\partial X} + \mathrm{Pr}\left(\frac{\partial^2 U}{\partial X^2} + \frac{\partial^2 U}{\partial Y^2}\right) \tag{3}$$

$$U\frac{\partial V}{\partial X} + V\frac{\partial V}{\partial Y} = -\frac{\partial P}{\partial Y} + \mathrm{Pr}\left(\frac{\partial^2 V}{\partial X^2} + \frac{\partial^2 V}{\partial Y^2}\right) + \mathrm{Ra}\,\mathrm{Pr}\,T \tag{4}$$

Energy:

$$U\frac{\partial T}{\partial X} + V\frac{\partial T}{\partial Y} = \frac{\partial^2 T}{\partial X^2} + \frac{\partial^2 T}{\partial Y^2} \tag{5}$$

The dimensionless variables in the above equations are defined as

$$(X, Y) = \frac{(x, y)}{H} \quad (U, V) = \frac{(u, v)}{\alpha/H} \quad P = \frac{p}{\rho(\alpha/H)^2} \quad T = \frac{(t - t_0)}{\Delta t} \tag{6}$$

using H, α/H, and $\Delta t = A_l$ (amplitude of the sinusoidal profile) as the characteristic scales for length, velocity, and temperature, respectively. The nondimensional parameters, Rayleigh number and Prandtl number, are defined as

$$\mathrm{Ra} = \frac{g\beta\,\Delta t\,H^3}{\nu\alpha} \quad \text{and} \quad \mathrm{Pr} = \frac{\nu}{\alpha} \tag{7}$$

For the boundary conditions for the above governing equations, the no-slip condition is imposed for all velocities on the walls, and the thermal boundary conditions are

$$\begin{aligned} T &= \sin(2\pi Y) && \text{at } X = 0 \\ T &= \varepsilon \sin(2\pi Y + \phi) && \text{at } X = \frac{1}{\mathrm{Ar}} \\ \frac{\partial T}{\partial n} &= 0 && \text{at } Y = 0 \quad \text{and} \quad Y = 1 \end{aligned} \tag{8}$$

where $\varepsilon = A_r/A_l$ is the amplitude ratio of the sinusoidal temperature on the right side wall to that on the left side wall, and $\mathrm{Ar} = H/L$ is the aspect ratio of the rectangular enclosure.

The fluid flow structure inside the enclosure is visualized by streamlines, and thus the stream functions (ψ) are defined as

$$\frac{\partial \psi}{\partial Y} = U \quad -\frac{\partial \psi}{\partial X} = V \tag{9}$$

Heat transfer across the enclosure is described by the Nusselt number. The local Nusselt number along the left and right side walls is defined as

$$\mathrm{Nu}_l = \left(-\frac{\partial T}{\partial n}\right)_{X=0} \quad \text{and} \quad \mathrm{Nu}_r = \left(-\frac{\partial T}{\partial n}\right)_{X=1/\mathrm{Ar}}. \tag{10}$$

In the heating half of the side wall, the fluid in the enclosure will gain heat from the side wall and thus $\mathrm{Nu} > 0$, but the fluid will lose heat in the cooling half of the side wall and hence $\mathrm{Nu} < 0$. The total heat transfer rate across the enclosure is the sum of the averaged Nusselt numbers along the heating halves of both vertical side walls, as described by the following average Nusselt number:

$$\overline{\mathrm{Nu}} = \int_{\text{heating half}} \mathrm{Nu}_l \, dY + \int_{\text{heating half}} \mathrm{Nu}_r \, dY \tag{11}$$

NUMERICAL PROCEDURE

The governing equations, Eqs. (2)–(5), are discretized by the finite-volume method (FVM) on a nonuniform grid system [19]. The third-order QUICK scheme and the second-order central difference scheme are implemented for the convection and diffusion terms, respectively. The set of discretized equations for each variable is solved by a line-by-line procedure, combining the tridiagonal matrix algorithm (TDMA) with the successive overrelaxation (SOR) iteration method. The coupling between velocity and pressure is solved by the SIMPLE algorithm [19]. The convergence criterion is that the maximal residual of all the governing equations is less than 10^{-6}.

In order to validate the numerical methods and codes of the present work, a recent, similar work by Bilgen and Yedder [10] was selected as the benchmark

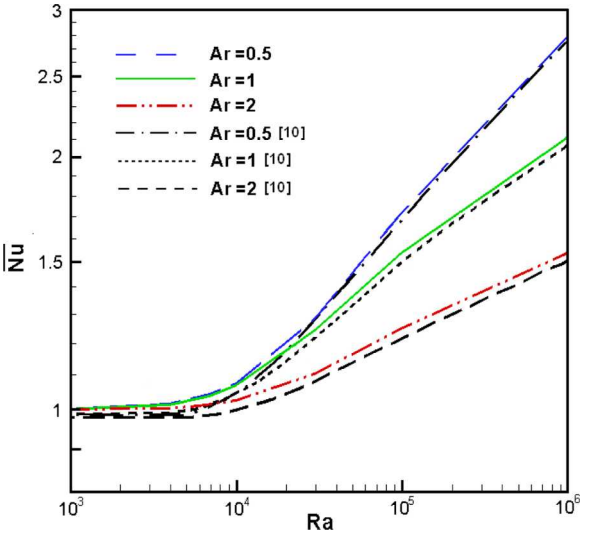

Figure 2. Comparisons of the normalized average Nusselt number at various aspect ratios between the present work and that of Bilgen and Yedder [10] (figure is provided in color online).

solution for comparison. Bilgen and Yedder considered the natural convection in an air-filled (Pr = 0.7) 2-D rectangular enclosure with three adiabatic walls and one side wall whose lower half is cooled but upper half is heated by a sinusoidal temperature profile. Figure 2 presents comparisons between the present results and those of Bilgen and Yedder for the normalized average Nusselt number of the enclosure within a wide Rayleigh number range ($Ra = 10^3$–10^6). It was observed that good agreement is achieved for various aspect ratios (Ar = 0.5, 1, 2).

RESULTS AND DISCUSSION

As indicated by above mathematic model, the natural convection under consideration is governed by five nondimensional parameters, two model parameters (Pr and Ra) from the governing equations and three boundary parameters (ε, ϕ, and Ar) from the boundary conditions. In the present study, the Prandtl number is kept constant at Pr = 0.7, and therefore main attention is paid to the effects of the remaining four parameters on the fluid flow and heat transfer characteristics in the enclosure. The effect of Rayleigh number (Ra) is first investigated at fixed boundary conditions, and then the effect of the boundary conditions, such as the amplitude ratio (ε), the phase deviation (ϕ), and the aspect ratio (Ar), are analyzed at various Rayleigh numbers.

Effect of Rayleigh Number (Ra)

In order to consider the effect of the Rayleigh number (Ra) only, the other boundary parameters are all kept constant at $\varepsilon = 1$, $\phi = 0$, Ar = 1, i.e., the natural convection in a square enclosure with the same temperature profiles on

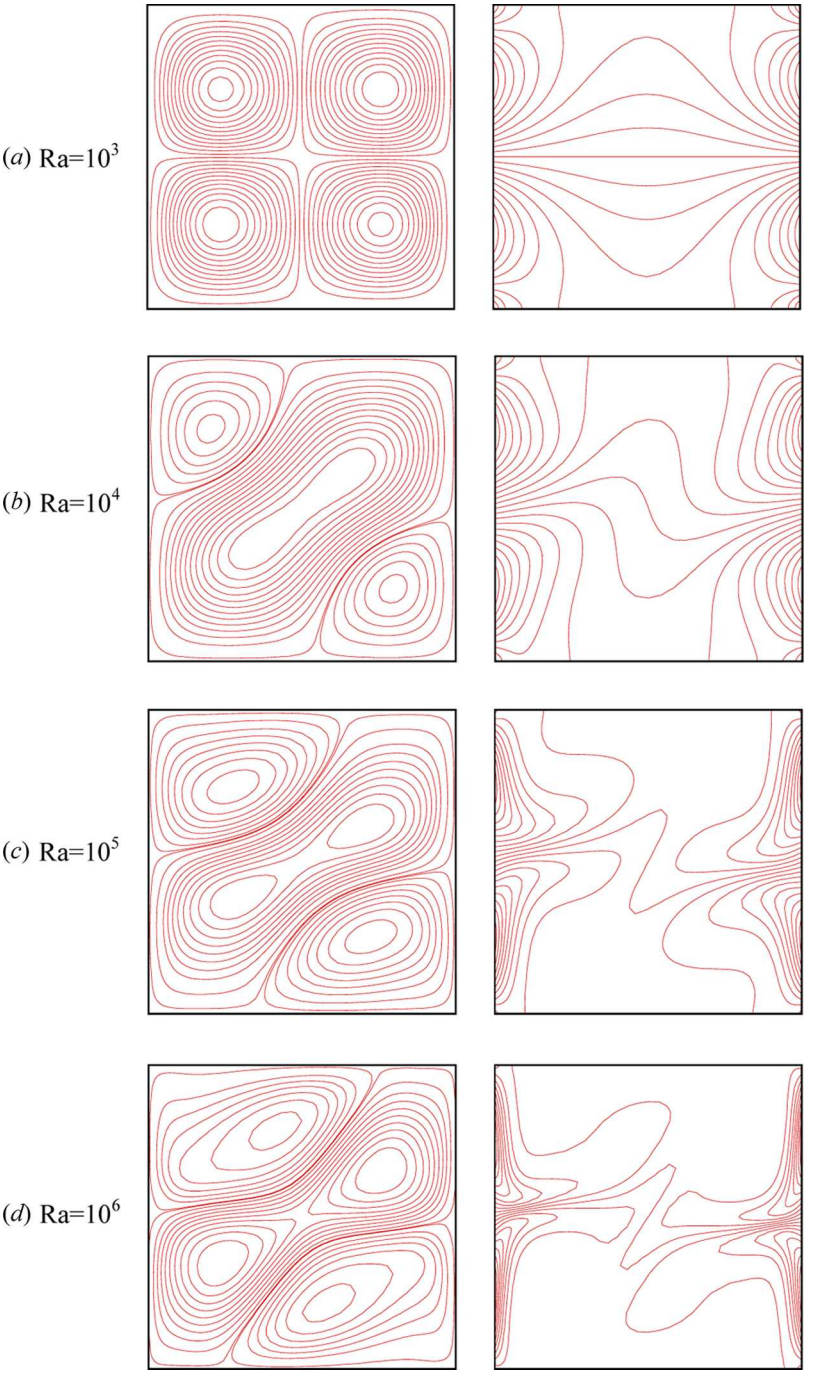

Figure 3. Effect of Rayleigh number on the streamlines (left) and isotherms (right) ($\varepsilon = 1$, $\phi = 0$, $\mathrm{Ar} = 1$) (figure is provided in color online).

the vertical side walls. Figure 3 shows the streamlines and isotherms at various Rayleigh numbers. At low Rayleigh number, $Ra = 10^3$, the flow in the enclosure is of 2×2 cellular structure with approximately vertical and horizontal symmetries about the middle of the enclosure and symmetry about its diagonals. The convection is very weak and hence the heat transfer is dominated by the conduction mechanism, as shown by the isotherms. As the Rayleigh number increases up to $Ra = 10^4$, a three-cellular flow structure is formed in the enclosure with one large diagonal cell and two smaller corner cells. Obviously, at this point the convection prevails, and thus the flow structure loses the vertical and horizontal symmetries but the diagonal symmetry remains so as to increase heat transfer. As the Rayleigh number continues to increase, the convection is strengthened, as seen by the fact that the inner kernel of the large diagonal cell breaks into two kernels, and also the corner cells expand. Accordingly, the heat transfer is enhanced as seen by the fact that the thermal boundary layers along the heating and cooling zones of the side walls shrink.

Figure 4 illustrates the variations of the local Nusselt number along the left side wall at various Rayleigh numbers. Because of the diagonally symmetric flow structure, the local Nusselt number along the right side wall is reverse and thus omitted. The Nu–Y curves are approximately of sinusoidal shape like the thermal boundary, which indicates that the local heat transfer is directly affected by the temperature distribution on the surface, i.e., larger heat transfer occurs where the temperature is higher. On the lower, heating half of the left side wall ($0 \leq Y \leq 0.5$), the fluid mainly gains heat and thus almost $Nu > 0$, and, in contrast, $Nu < 0$ is observed on the upper, cooling half of the left side wall ($0.5 \leq Y \leq 1$), but reverse heat transfer occurs near the edges of the heating and cooling zones due to the nonuniform temperature distribution. On the other hand, heat transfer in the

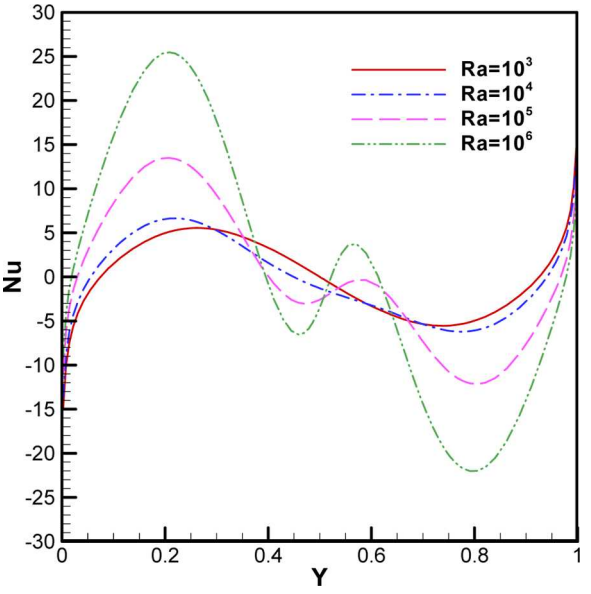

Figure 4. Effect of Rayleigh number on the local Nusselt number of the left wall ($\varepsilon = 1$, $\phi = 0$, $Ar = 1$) (figure is provided in color online).

enclosure is increased as the Rayleigh number increases, as seen as the amplitude of the Nu–Y curve increases significantly. It is worth noting that the local Nusselt number distributions are not symmetric along the horizontal centerline ($Y = 0.5$) like the boundary temperature distributions. The maximal local Nusselt number on the lower heating half is larger than the minimal value on the upper half, i.e., more heat is transferred from the lower heating half than from the upper half of the left side wall. This is consistent with the flow structure, as a larger cell is formed along the lower heating half than along the upper cooling half.

Effect of Amplitude Ratio (ε)

Now consider the amplitude effect of the sinusoidal temperature profile along the right side wall on the heat transfer across the enclosure at various Rayleigh numbers. The other parameters are kept constant at $\mathrm{Ar} = 1$ and $\phi = 0$. The temperature amplitude ratio (ε) of the right side wall to the left side wall is varied from 0 to 1, and the adiabatic condition on the right side wall is also considered here for comparison. Figure 5 presents the variations of the average Nusselt number ($\overline{\mathrm{Nu}}$) of the enclosure in terms of Rayleigh number (Ra) at various amplitude ratios (ε). Obviously, the average Nusselt number is increased as Rayleigh number increases for each amplitude ratio case. On the other hand, the average Nusselt number is also increased as the amplitude ratio increases from 0 to 1 at various Rayleigh numbers, but the increasing tendency is augmented as Rayleigh number increases. The figure shows that the heat transfer is increased as the amplitude ratio (ε) increases, and that the heat transfer for cases $\varepsilon > 0$ is higher than the case $\varepsilon = 0$, which is equivalent to

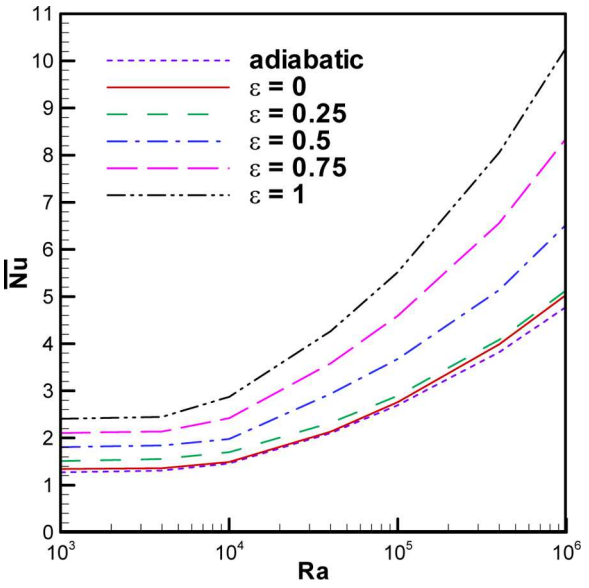

Figure 5. Effect of the amplitude ratio (ε) on the average Nusselt numbers ($\phi = 0$ and $\mathrm{Ar} = 1$) (figure is provided in color online).

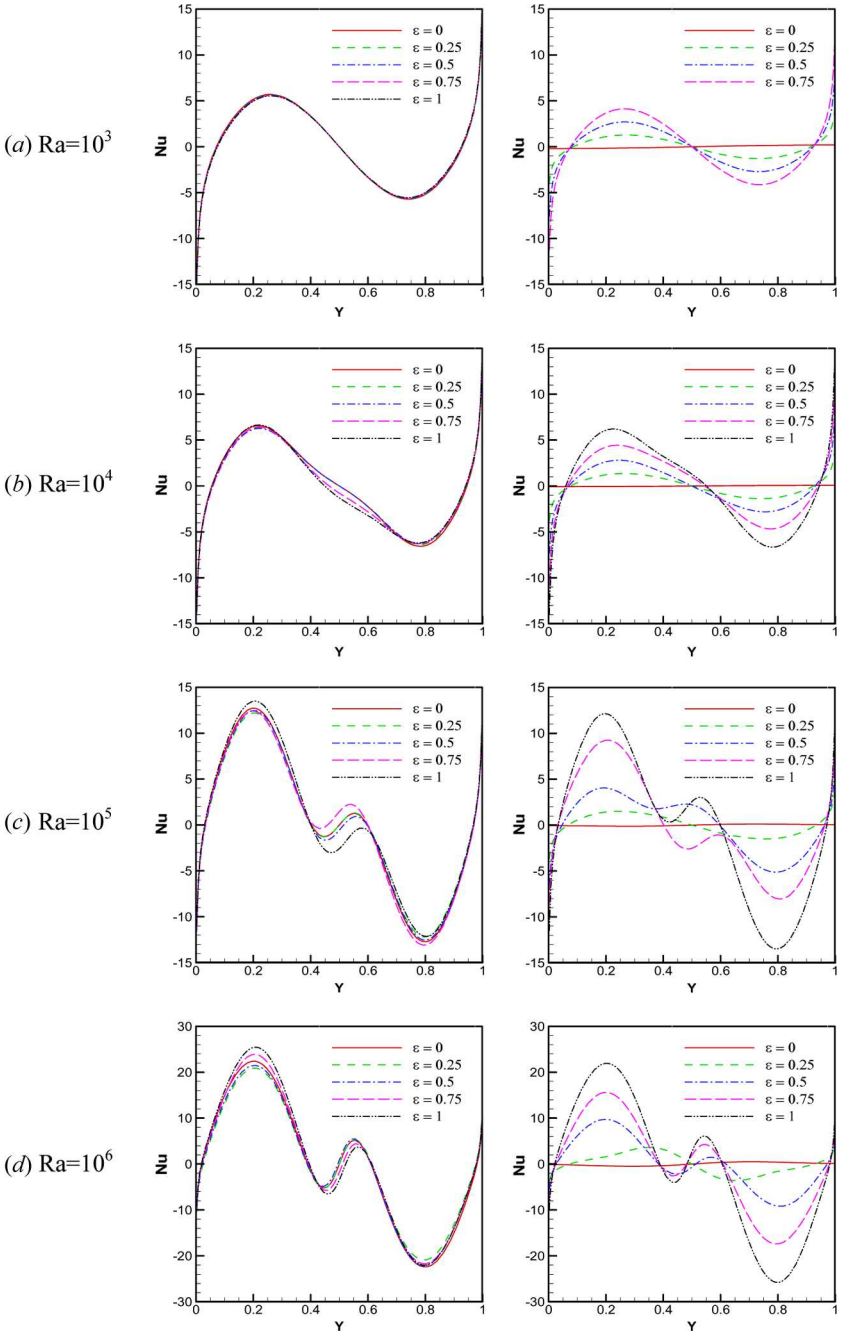

Figure 6. Effect of the amplitude ratio (ε) on the local Nusselt numbers of the left (left) and right (right) side walls ($\phi = 0$ and $\mathrm{Ar} = 1$) (figure is provided in color online).

the adiabatic case. This means that the nonuniform or sinusoidal temperature distribution on the side wall is beneficial for improving heat transfer, as compared to the case where the wall is kept at uniform or constant temperature ($\varepsilon = 0$) and also the case where the wall is insulated.

In order to better understand and assess the above effect of the amplitude ratio on the total heat transfer, Figure 6 presents the detailed distributions of the local Nusselt number along the Y coordinate for both the left and right side walls at various Rayleigh numbers. First, it is observed that the heat transfer on both side walls is significantly increased as Ra increases from 10^3 to 10^6. Second, it is interesting to find that the heat transfer of the left side wall is nearly not affected by the variation of temperature amplitude of the right side wall. The curves Nu–Y for the left side wall at each Rayleigh number are nearly the same as the amplitude ratio (ε) changes. Third, the heat transfer of the right side wall is obviously increased as its temperature amplitude ratio varies from 0 to 1, and the increasing tendency becomes serious as Ra increases. This implies that the variation of temperature amplitude of the right wall can only change the heat transfer on its own surface; it cannot affect the heat transfer on the other side wall.

The inherent reason for the effect of temperature amplitude can be explored by examning the microscopic flow patterns and temperature distributions within the enclosure. Figure 7 depicts the changes of the streamlines and isotherms in terms of the amplitude ratio of the temperature on the right wall (ε) for $\mathrm{Ra} = 10^5$. When the right side wall is kept at constant temperature ($\varepsilon = 0$), the streamlines show that two symmetric cells are formed in the upper and lower halves of the enclosure, and the isotherms show that the temperature variations are mainly within a thin region near the left side wall, with the remaining region near the right side wall of uniform or mean temperature. Therefore, heat transfer occurs only at the left side wall and not at the right side wall. As the amplitude ratio increases up to the level $\varepsilon = 0.25$, a four-cellular flow structure forms in the enclosure, with two main circulations near the left side wall and two secondary circulations near the right side wall. Accordingly, the isotherms along the left side wall are nearly the same as before, and

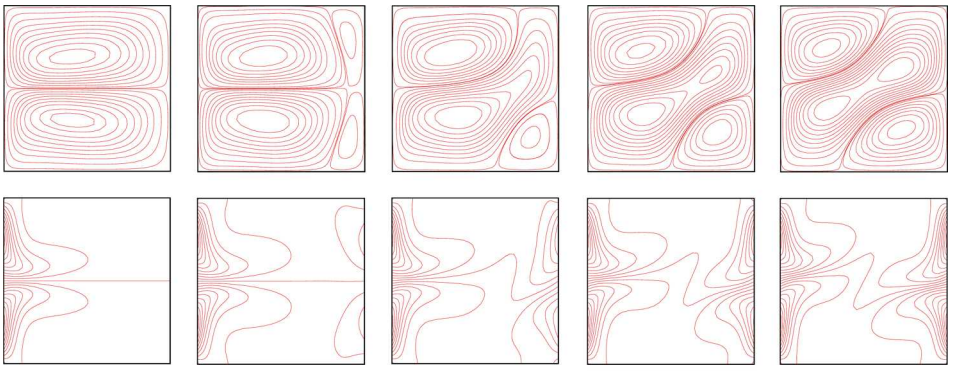

Figure 7. Effect of the amplitude ratio (ε) on the streamlines (top) and isotherms (bottom) ($\phi = 0$, $\mathrm{Ar} = 1$, $\mathrm{Ra} = 10^5$) (figure is provided in color online).

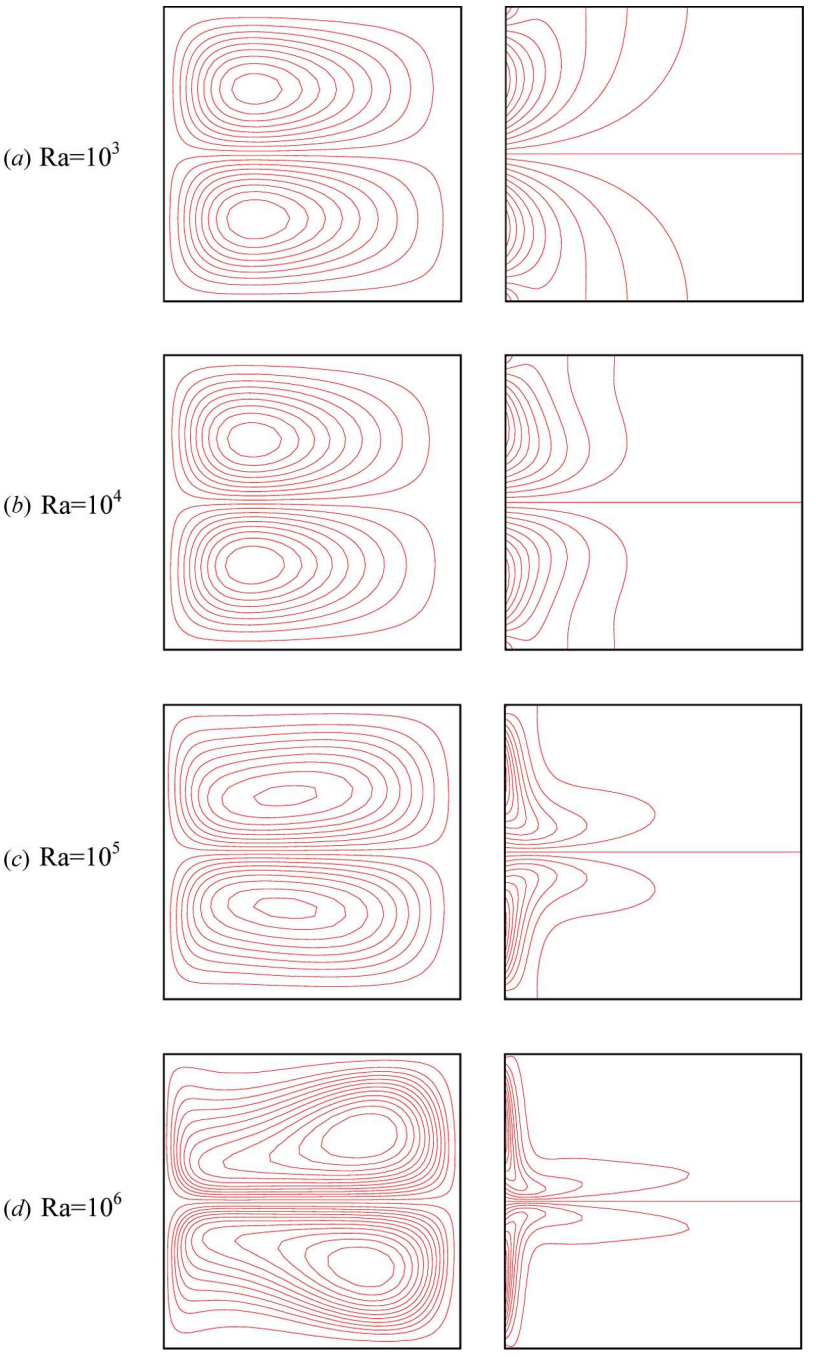

Figure 8. Streamlines (left) and isotherms (right) for cases that $\varepsilon = 0$ and adiabatic right side wall ($\phi = 0$ and $\mathrm{Ar} = 1$) (figure is provided in color online).

hence the heat transfer across the surface is kept fixed. But the temperature along the right side wall is not uniform any more, as observed where a small number of isotherms appear near the surface, which results in a weak heat transfer. As ε increases further, the flow structure changes to three cells, as seen where the bottom secondary cell expands, the upper main cell shrinks, and the top secondary cell is combined with the lower main cell. At $\varepsilon = 1$, the three-cellular flow structure is of diagonal symmetry, with one large diagonal cell and two small corner cells. Simultaneously, more and more isotherms appear along the right side wall and thus heat transfer across the right side wall increases. However, during the course of increasing ε, the flow along the left side wall is nearly invariant, as seen by streamlines where the upper half of the surface is always flushed by a downward cold cell and the lower half of the surface is flushed by a upward hot cell. Influenced by the flow structure, the temperature distributions indicated by isotherms along the left side wall are invariant, and thus heat transfer is kept invariant.

In order to illustrate the low heat transfer for the case where the right side wall is kept at a uniform temperature ($\varepsilon = 0$) or at adiabatic condition, Figure 8 shows the streamlines and isotherms at various Rayleigh numbers. The streamlines indicate that the flow structure is always of two symmetric cells. Isotherms show that the fluid temperature changes only along the active left side wall and always remains at constant or uniform (mean) temperature along the right side wall. This means the right side wall is always inert. However, in the case where two sinusoidally varying temperature distributions are imposed on the side walls, both side walls are active and hence the heat transfer is enhanced.

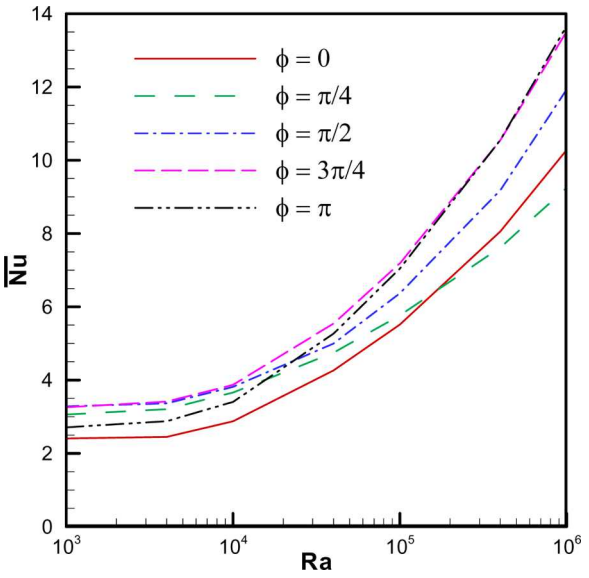

Figure 9. Effect of the phase deviation (ϕ) on the average Nusselt number ($\varepsilon = 1$ and $Ar = 1$) (figure is provided in color online).

Effect of Phase Deviation (ϕ)

Figure 9 shows the variations of the average Nusselt number across the enclosure in terms of Rayleigh number at various phase deviations ($\phi = 0, \pi/4, \pi/2, 3\pi/4, \pi$) of the temperature profiles between the left and right side walls, and

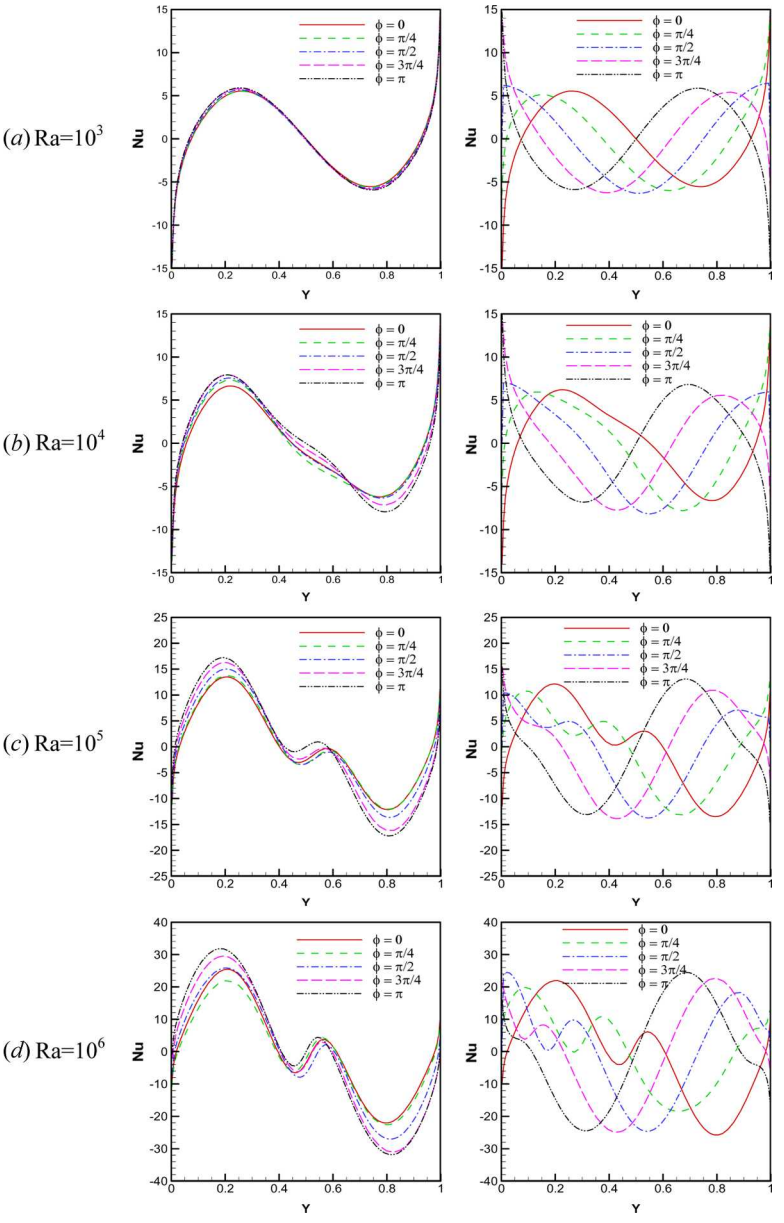

Figure 10. Effect of the phase deviation (ϕ) on the local Nusselt numbers of the left (left) and right (right) side walls ($\varepsilon = 1$ and $Ar = 1$) (figure is provided in color online).

the other parameters are kept constant at $\varepsilon = 1$ and $\mathrm{Ar} = 1$. It is found that the average Nusselt number ($\overline{\mathrm{Nu}}$) is always increased as the Rayleigh number (Ra) increases for each phase deviation (ϕ). Although no consistent tendency is observed for the effect of phase deviation, it is obvious that the average Nusselt number is basically the lowest for the case $\phi = 0$. As the phase deviation increases up to $\phi = \pi/4$, the average Nusselt number is enhanced within a wide range of the Rayleigh numbers ($\mathrm{Ra} \leq 10^5$) but slightly lowered at $\mathrm{Ra} = 10^6$. As the phase deviation increases further, such as to $\phi = \pi/2$, the heat transfer is enhanced within the whole range of the Rayleigh numbers, and reaches the highest as the phase deviation is increased up to $\phi = 3\pi/4$. Then, the average Nusselt number begins to decrease as the phase deviation increases further, such as to $\phi = \pi$.

Figure 10 shows the effect of the phase deviation on the local Nusselt number along the Y coordinates of the left and right side walls. It is found that the heat transfer of the left side wall is not so much influenced as the right side wall by the phase change of the temperature profile on the right side wall, as seen that the local Nusselt number distribution on the left side wall is slightly affected by the phase change. However, the local Nusselt number distribution on the right side wall is significant by affected by the phase change, as seen that the heating zone moves upward and the cooling zone moves downward as the phase deviation (ϕ) changes from 0 to π.

Figure 11 illustrates the variations of the streamlines and isotherms as the phase deviation changes from $\phi = 0$ to $\phi = \pi$ at $\mathrm{Ra} = 10^5$. At $\phi = 0$, the flow is of three-cellular structure with one large diagonal cell and two smaller corner cells of identical sizes. As the phase deviation increases, the size of the upper corner cell is enlarged but the size of the lower corner cell is decreased. At $\phi = \pi$, the lower corner cell disappears, and the flow structure is of two identical cells in the halves of the enclosure. During the variation course of the phase deviation, the isotherms along the left side wall are nearly retained, but the isotherm distributions along the right side wall are changed. Therefore, the heat transfer on the left side wall is kept fixed, but that on the right side wall is varied.

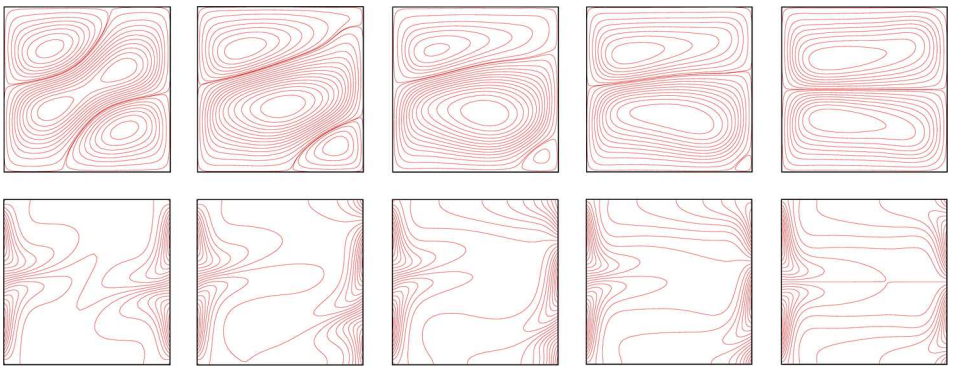

Figure 11. Effect of the phase deviation (ϕ) on the streamlines (top) and isotherms (bottom) ($\varepsilon = 1$, $\mathrm{Ar} = 1$, and $\mathrm{Ra} = 10^5$) (figure is provided in color online).

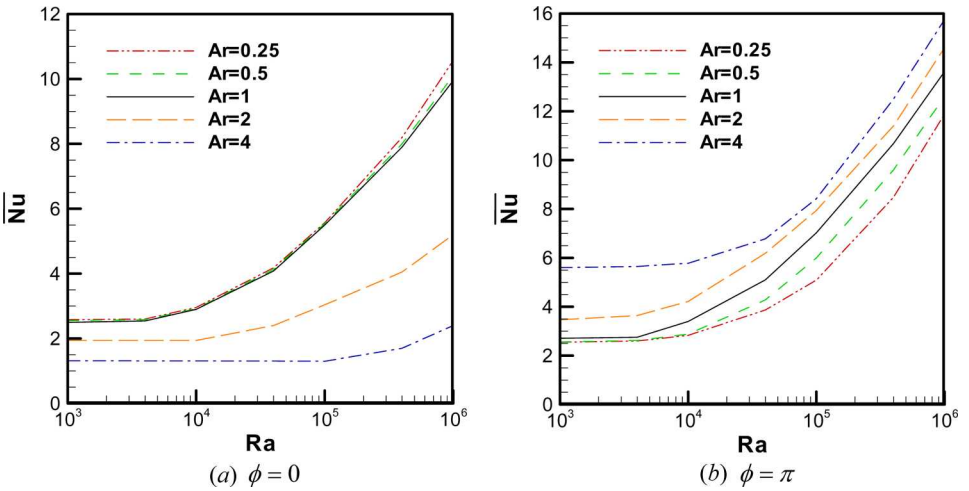

Figure 12. Effect of the aspect ratio on the average Nusselt numbers (figure is provided in color online).

Effect of Aspect Ratio (Ar)

In order to investigate the effect of the aspect ratio on the heat transfer across the enclosure with two sinusoidal temperature profiles of the same amplitude ($\varepsilon = 1$) on the vertical sidewalls, Figure 12 plots the variations of the average Nusselt number in terms of Rayleigh number at various aspect ratios ($\mathrm{Ar} = 0.25, 0.5, 1, 2, 4$) for two cases, one of the same phase ($\phi = 0$) and the other of the reversed phase ($\phi = \pi$). When the two sinusoidal temperatures are of the same phase ($\phi = 0$), as seen in Figure 12*a*, the average Nusselt number of the enclosure is first kept invariant as the aspect ratio (Ar) is less than unity. However, if the aspect ratio is larger than unity, the average Nusselt number is decreased as the aspect ratio is increasing. This means that it is not beneficial to heat transfer to have a narrow enclosure with two sinusoidal temperatures of the same phase. When the two sinusoidal temperatures are of the reversed phase ($\phi = \pi$), as presented in Figure 12*b*, the average Nusselt number of the enclosure is always increased as the aspect ratio is increasing, which means that heat transfer can be improved by marrowing the enclosure.

CONCLUSIONS

The present work studied numerically a 2-D steady and laminar natural convection in an air-filled rectangular enclosure with two spatially varying sinusoidal temperature distributions on the vertical left and right side walls. Main attention has been focused on the effect of the main factors, including the Rayleigh number (Ra), the amplitude ratio (ε), and the phase deviation (ϕ) of the sinusoidal temperature distribution between the right and left side walls, and the aspect ratio (Ar) of the enclosure, on the fluid flow and heat transfer characteristics. Main conclusions are as follows.

1. The heat transfer is increased as the amplitude ratio (ε) increases from 0 to 1. This means that the nonuniformly sinusoidal temperature distribution on the

side wall is beneficial for improving heat transfer as compared to the case where the wall is kept at uniform temperature ($\varepsilon = 0$).
2. The heat transfer is the worst if the temperature profiles on both side walls are of same phase ($\phi = 0$), and reaches the highest when the phase deviation $\phi = 3\pi/4$.
3. The variation of the amplitude or phase of the sinusoidal temperature distribution on one side wall mainly affects the heat transfer on its own surface; it has little effect on the other side wall.
4. The average Nusselt number of the enclosure is decreased with the aspect ratio when the two sinusoidal temperatures are of the same phase ($\phi = 0$), but is increased if the sinusoidal temperatures are of reversed phase ($\phi = \pi$).

REFERENCES

1. S. Ostrach, Natural Convection in Enclosures, *ASME J. Heat Transfer*, vol. 110, pp. 1175–1190, 1988.
2. D. Poulikakos, Natural Convection in a Confined Fluid-Filled Space Driven by a Single Vertical Wall with Warm and Cold Regions, *ASME J. Heat Transfer*, vol. 107, pp. 867–876, 1985.
3. C. C. Jahnke, V. Subramanyan, and D. T. Valentine, On the Convection in an Enclosed Container with Unstable Side Wall Temperature Distributions, *Int. J. Heat Mass Transfer*, vol. 41, pp. 2307–2320, 1998.
4. W. S. Fu, C. C. Tseng, and Y. C. Chen, Natural Convection in an Enclosure with Non-uniform Wall Temperature, *Int. Commun. Heat Mass Transfer*, vol. 21, pp. 819–828, 1994.
5. P. H. Oosthuizen, Natural Convective Heat Transfer across a Cavity with Cooled Top Surface application to a Simple Dryer, *Proc. ASME Heat Transfer Division, Single and Multiphase Convective Heat Transfer*, vol. 145, pp. 1–11, 1990.
6. B. V. R. Kumar and P. Singh, Effect of Thermal Stratification on Free Convection in a Fluid-Saturated Porous Enclosure, *Numer. Heat Transfer A*, vol. 34, pp. 343–356, 1998.
7. B. V. R. Kumar and Shalini, Natural Convection in a Thermally Stratified Wavy Vertical Porous Enclosure, *Numer. Heat Transfer A*, vol. 43, pp. 753–776, 2003.
8. M. Sathiyamoorthy, T. Basak, S. Roy, and I. Pop, Steady Natural Convection Flows in a Square Cavity with Linearly Heated Side Wall(s), *Int. J. Heat Mass Transfer*, vol. 50, pp. 766–775, 2007.
9. M. Sathiyamoorthy, T. Basak, S. Roy, and I. Pop, Steady Natural Convection Flows in a Square Cavity Filled with a Porous Medium for Linearly Heated Side Wall(s), *Int. J. Heat Mass Transfer*, vol. 50, pp. 1892–1901, 2007.
10. E. Bilgen and R. B. Yedder, Natural Convection in Enclosure with Heating and Cooling by Sinusoidal Temperature Profiles on One Side, *Int. J. Heat Mass Transfer*, vol. 50, pp.139–150, 2007.
11. I. E. Sarris, I. Lekakis, and N. S. Vlachos, Natural Convection in a 2D Enclosure with Sinusoidal Upper Wall Temperature, *Numer. Heat Transfer A*, vol. 42, pp. 513–530, 2002.
12. Y. Varol, H. F. Oztop, and I. Pop, Numerical Analysis of Natural Convection for a Porous Rectangular Enclosure with Sinusoidally Varying Temperature Profile on the Bottom Wall, *Int. Commun. Heat Mass Transfer*, vol. 35, pp. 56–64, 2008.
13. N. H. Saeid and Y. Yaacob, Natural Convection in a Square Cavity with Spatial Side-Wall Temperature Variation, *Numer. Heat Transfer A*, vol. 49, pp. 683–697, 2006.

14. N. H. Saeid and A. A. Mohamad, Natural Convection in a Porous Cavity with Spatial Sidewall Temperature Variation, *Int. J. Numer. Meth. Heat Fluid Flow*, vol. 15, pp. 555–566, 2005.
15. T. Basak, S. Roy, and A. R. Balakrishnan, Effects of Thermal Boundary Conditions on Natural Convection Flows within a Square Cavity, *Int. J. Heat Mass Transfer*, vol. 49, pp. 4525–4535, 2006.
16. A. Dalal and M. K. Das, Natural Convection in a Rectangular Cavity Heated from Below and Uniformly Cooled from the Top and Both Sides, *Numer. Heat Transfer A*, vol. 49, pp. 301–322, 2006.
17. A. Dalal and M. K. Das, Numerical Study of Laminar Natural Convection in a Complicated Cavity Heated from Top with Sinusoidal Temperature and Cooled from Other Sides, *Comput. Fluids*, vol. 36, pp. 680–700, 2007.
18. A. Dalal and M. K. Das, Laminar Natural Convection in an Inclined Complicated Cavity with Spatially Variable Wall Temperature, *Int. J. Heat Mass Transfer*, vol. 48, pp. 3883–3854, 2005.
19. S. V. Patankar, *Numerical Heat Transfer and Fluid Flow*, Hemisphere, London, 1980.